All-Order Polarization-Mode Dispersion (PMD) Compensation via Virtually Imaged Phased Array (VIPA)-Based Pulse Shaper

Houxun Miao, *Student Member, IEEE*, Andrew M. Weiner, *Fellow, IEEE*, Leo Mirkin, and Peter J. Miller

Abstract—**We demonstrated all-order polarization-mode dispersion compensation using a virtually imaged phased-array-based transmission pulse shaper. We reduced the pulsewidth of polarization-mode dispersed pulses from more than 100 ps to their original 15 ps.**

Index Terms—**Optical fiber communication, polarization-mode dispersion (PMD), ultrafast pulse shaping, virtually imaged phased array (VIPA).**

I. Introduction

As BIT rates continue to increase, polarization-mode dispersion (PMD) has emerged as a key factor limiting high-speed transmission in optical fiber links [1]. PMD arises from the random birefringences in optical fibers due to the imperfect symmetry in the fiber core. This results in time-stochastic and wavelength-dependent variation of the states of polarization (SOPs) and delays, which may degrade the system capacity. Generally, PMD is studied in a Taylor series expansion framework in terms of first-order PMD, second-order PMD, etc. Traditional optical PMD compensators are typically restricted to the low-order approximation (first- and second-order) [2], [3]. However, as the bandwidth of telecommunication systems increases, compensation of all-order PMD effects becomes increasingly important [4]. In our previous work [5], we demonstrated experimental all-order PMD compensation of subpicosecond pulses distorted by a PMD module with mean differential group delay (DGD) $\sim$7 times the pulsewidth via wavelength-parallel characterization and compensation of the frequency-dependent Jones matrix associated with PMD. A grating-based wavelength-parallel polarimeter [6] and a grating-based pulse shaper (or equivalently, a wavelength-parallel processor) [7] were used for the Jones matrix characterization and correction, respectively. The mean DGD in these subpicosecond experiments was $\sim$5 ps, and the sensing element and control element spacings corresponded to $\sim$10 GHz. These parameters are appropriate for high bit rate systems (e.g., 640 Gb/s), but not for 40-Gb/s systems where we are interested in mean DGDs of several tens of picoseconds for all-order compensation experiments. In this work, we introduce a virtually imaged phased array (VIPA)-based [8], [9] polarimeter and pulse shaper with control element spacings corresponding to only 1.6 GHz for wavelength-parallel Jones matrix sensing and correction. We demonstrate full compensation of $\sim$15-ps optical pulses, distorted by all-order PMD effects to more than 100 ps, by using a VIPA-based transmission pulse shaper incorporating a specially designed four-layer liquid crystal modulator (LCM) array. Our results demonstrate the feasibility of scaling our all-order PMD compensation concept to optical bandwidths consistent with near-term lightwave communication rates.

Manuscript received October 18, 2007; revised December 6, 2007. This work was supported in part by the National Science Foundation under Grant 0501366-ECS.

H. Miao and A. M. Weiner are with the School of Electrical and Computer Engineering, Purdue University, West Lafayette, IN 47907-1285 USA (e-mail: hmiao@purdue.edu; amw@ecn.purdue.edu).

L. Mirkin and P. J. Miller are with CRI Inc., Woburn, MA 01801 USA (e-mail: LMirkin@cri-inc.com; PJMiller@cri-inc.com).

Color versions of one or more of the figures in this letter are available online at http://ieeexplore.ieee.org.

Digital Object Identifier 10.1109/LPT.2008.918893

II. Experimental Setup and Results

The PMD compensation concept here is the same as that in [5]. As described in detail in [5], full all-order PMD compensation can be achieved by correcting the frequency-dependent Jones matrix of the fiber link to a frequency-independent constant matrix. The frequency-dependence of the Jones matrix can be completely characterized with an arbitrary, frequency-independent input SOP by sequentially transforming the input SOP into four different SOPs by using a pair of switchable ferroelectric liquid crystal (FLC) retarders, launching them into the fiber link and measuring the corresponding output SOP spectra with a wavelength-parallel polarimeter. The measured frequency-dependent Jones matrix can be corrected to a frequency-independent matrix with a transmission pulse shaper incorporating a specially designed four-layer LCM array. After that, all-order PMD effects are fully compensated.

Fig. 1 shows our experimental setup. A passively mode-locked fiber ring laser followed by a bandpass filter [$\sim$40-GHz full-width at half-maximum (FWHM)] and an erbium-doped fiber amplifier (EDFA) is used to produce $\sim$15-ps pulses with 50-MHz repetition rate and 1550.7-nm center wavelength. Another bandpass filter with 4-nm FWHM is used to filter out the ASE noise introduced by the EDFA. Although its use is not required, a polarization controller (PC) is available for arbitrary adjustment of the input SOP. We use two switchable FLC retarders to switch the input SOP among four different SOP states. Each FLC acts as a quarter wave retarder at 1550 nm and has two stable optic axis orientations separated by approximately 45°. The switching time between axes is $\sim$70 μs. The orientations of the axes of the two FLCs

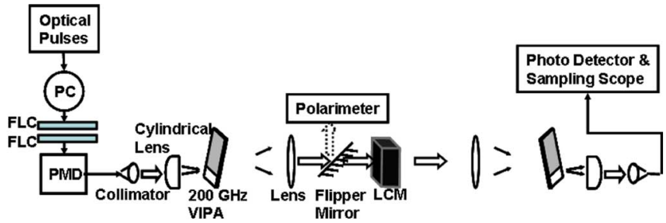

Fig. 1. Experimental setup. The polarimeter consists of a pair of FLC retarders, a polarizer and a 256-pixel linear InGaAs detector array. The block arrows indicate the direction of the signal flow.

are 0° (state 0) – 45° (state 1) and 45° (state 0) – 90° (state 1), respectively. Consequently, the SOP transformations are denoted by the combination of the FLC states as 00, 01, 10, 11. The signal is then connected to the PMD module consisting of three homemade PMD emulators connected via PCs. The three PMD emulators consist of five, eight, and six PM fibers spliced at various angles, with an overall estimated mean DGD of 42 ps. The distorted signal is launched into a VIPA-based transmission pulse shaper incorporating a four-layer LCM for PMD compensation. Each LCM layer functions as a linear retarder array (128 independently addressable pixels) with specified fast axis and arbitrarily adjustable retardance. The orientations of the LCM layers are 0°–45°–0°–90°, respectively. The free-spectral ranges (FSRs) of the VIPAs are 200 GHz and the incident angle to the VIPA is $\sim$2.5°. A flipper mirror is used to integrate the wavelength-parallel polarimeter [6] to the pulse shaper. For simultaneous SOP sensing and PMD compensation, one can use a nonpolarizing beam splitter to direct part of the light into the polarimeter as demonstrated in [5]. A 50-GHz fast photodetector and a sampling oscilloscope are used to directly observe the distorted and restored pulses.

Fig. 2 shows an example of four Poincare sphere plots (corresponding to the four FLC states) of SOP spectra distorted by PMD. The average angles between states 00-01, 00-10, 00-11, 01-10, 01-11, 10-11 are 10.9°, 100.2°, 111.8°, 105.4°, 101.4°, and 120.2°. As indicated in [5], two output SOP spectra whose relative angle is closest to 90° on the Poincare sphere should be selected for accurate Jones matrix characterization. Note that with the proposed configuration of FLC retarders, there are always at least two FLC states yielding output SOPs separated by an angle in the range between 60° and 120° on the Poincare sphere. This guarantees that Jones matrix characterization will be accurate enough. We first select the data from 00-10 states for control of our PMD compensator. Fig. 3 shows the temporal intensity profiles (average trace over 128 data sets) of the optical pulses before and after PMD compensation. The peak intensity of the pulse after compensation is normalized to 1. The pulse without PMD effects is plotted with the restored pulse in Fig. 3(B) for comparison. After compensation, the pulse is compressed from more than 100 ps (10% intensity) to $\sim$15 ps (FWHM). Compared to the initial pulse, almost perfect compensation has been achieved. To demonstrate the robustness of our PMD sensing/compensation system, we now repeat the experiment with identical PMD but using the data from the 10-11 FLC sensing states (the angle between which is $\sim$120°). Fig. 4 shows the restored pulse together with the initial pulse [the distorted pulse is the same as in Fig. 3(A)]. Again, perfect compensation has been achieved. During the above measurement, the FLC retarders at the input side are held in a stable state.

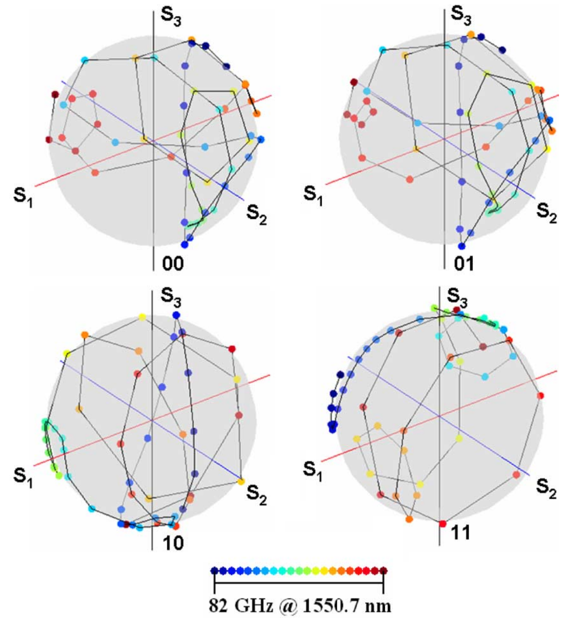

Fig. 2. Output SOP spectra corresponding to the 4 FLC states: 00, 01, 10, 11. Each point corresponds to a measured SOP vector at a specified pixel of the detector array (corresponding to a wavelength component).

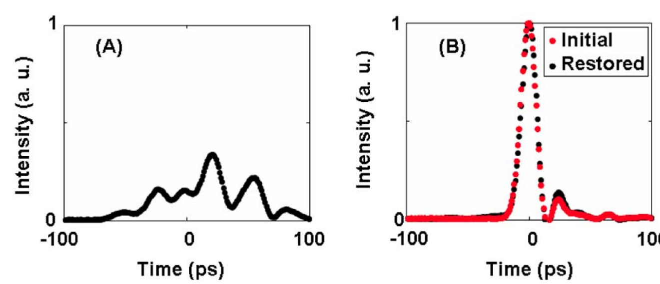

Fig. 3. PMD compensation results. (A) Distorted pulse; (B) restored and initial pulses.

By adjusting the PC at the input side and the PCs between the PM emulators, we tried the experiments with more than ten independent PMD profiles. Each time, after PMD compensation, we can compress the pulses to $\sim$15 ps in duration, without any apparent distortion. Fig. 5 shows the distorted and restored pulses of another PMD compensation trial.

As in [5], our PMD compensation technique is compatible with simultaneous real-time sensing and compensation because once the compensator is set, it works for any input SOP. Here we more critically study the transient effects of the FLC retarders by looking at persistent traces of the distorted and restored pulses while keeping the FLCs switching. Fig. 6 shows the measured persistent traces corresponding to Fig. 3. Fig. 6(A) shows the initial pulse while the FLC is kept stable. Fig. 6(B) shows the PMD distorted pulse while the FLC is switching at a rate of 20 Hz. Two stable states are clearly depicted. Fig. 6(C) shows the distorted pulse while the FLC is switching at a rate of 2 kHz. Transient effects between the two stable states are clearly displayed. Fig. 6(D) shows the restored pulse after PMD

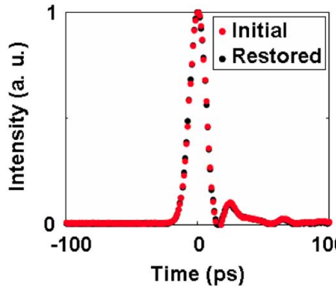

Fig. 4. PMD compensation result with 10-11 FLC states selected.

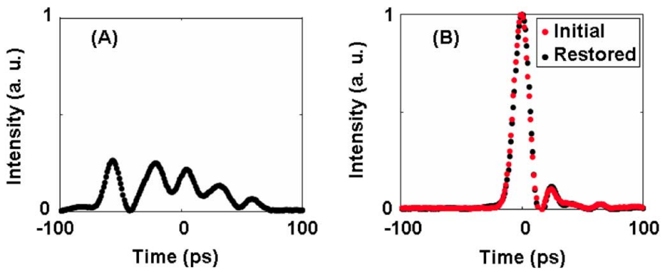

Fig. 5. Distorted (A) and restored pulses (B).

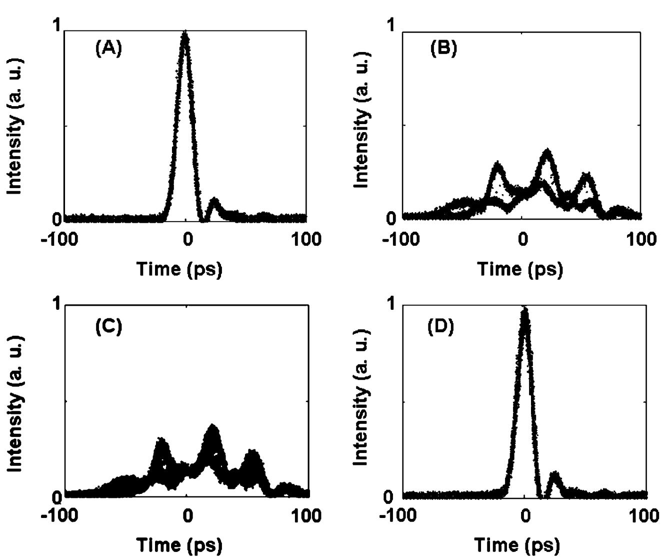

Fig. 6. Persistent traces of the initial pulse (A), PMD distorted pulse with the FLCs switching at a rate of 20 Hz (B), distorted pulse with the FLCs switching at 2 kHz (C) and the restored pulse with the FLC switching at 2 kHz (D).

compensation [corresponding to Fig. 3(B)] while the FLC kept switching at a rate of 2 kHz. The restored pulse is very close to the initial pulse, except that there is a ~5% power fluctuation at the peak. We attribute this fluctuation to transient loss introduced by the FLC retarders (we see the same fluctuation for the initial undistorted pulse when the FLC retarders are kept switching). Based on ~10 experimental trials, we did not see any other degradation induced by FLC switching except these small power fluctuations. These data provide evidence of the feasibility of continuous in-line sensing based on switching of the launching polarization.

III. Conclusion and Discussion

We have demonstrated all-order compensation of ~15-ps pulses distorted by all-order PMD effects to more than 100 ps via a VIPA-based transmission pulse shaper with a resolution of ~1.6 GHz/pixel. The amount of PMD that can be accurately sensed and fully compensated is only limited by the resolution of the polarimeter and of the pulse shaper, respectively. A conservative estimate, consistent with very high-quality compensation, is that mean DGD should remain below 1/16 of the inverse of the spectral resolution. In the current experiment with ~42-ps mean DGD, we are approximately at this limit, which should be sufficient to handle most long-haul systems.

Note that since multiple FSRs overlap in space in a VIPA-based pulse shaper configuration, the proposed experimental setup (VIPAs with 200-GHz FSR) is only suitable for PMD compensation of two 40-Gb/s wavelength-division-multiplexing (WDM) channels with 100-GHz channel spacing or for one 100-Gb/s channel with 200-GHz channel spacing. In the future, wideband PMD compensation of tens of WDM channels may be possible in a single apparatus by using new pulse shaper geometries based on spectral dispersion in two dimensions. Such two-dimensional spectral dispersion has been demonstrated using a combined grating-VIPA arrangement [10], which allows simultaneous realization of broad spectral coverage and high spectral resolution.

Acknowledgment

The authors acknowledge D. E. Leaird and S. X. Wang for their contribution.

References

[1] H. Kogelnik, R. M. Jopson, and L. E. Nelson, “Polarization Mode Dispersion,” in *Optical Fiber Telecommunications IVB-Systems and Impairments*, I. P. Kaminow and T. Li, Eds. New York: Academic, 2002, p. 723.

[2] F. Buchali and H. Büllow, “Adaptive PMD compensation by electrical and optical techniques,” *J. Lightw. Technol.*, vol. 22, no. 4, pp. 1116–1126, Apr. 2004.

[3] H. Miao and C. Yang, “Feed-forward polarization-mode dispersion compensation with four fixed differential group delay elements,” *IEEE Photon. Technol. Lett.*, vol. 16, no. 4, pp. 1056–1058, Apr. 2004.

[4] P. B. Phua, H. A. Haus, and E. P. Ippen, “All-frequency PMD compensator in feedforward scheme,” *J. Lightw. Technol.*, vol. 22, no. 5, pp. 1280–1289, May 2004.

[5] H. Miao, A. M. Weiner, L. Mirkin, and P. J. Miller, “Broadband all-order polarization mode dispersion compensation via wavelength by wavelength Jones matrices correction,” *Opt. Lett.*, vol. 32, pp. 2360–2362, Aug. 2007.

[6] S. X. Wang and A. M. Weiner, “A complete spectral polarimeter design for lightwave communication systems,” *J. Lightw. Technol.*, vol. 24, no. 11, pp. 3982–3991, Nov. 2006.

[7] A. M. Weiner, “Femtosecond pulse shaping using spatial light modulators,” *Rev. Sci. Instrum.*, vol. 71, no. 5, pp. 1929–1960, May 2000.

[8] M. Shirasaki, “Large angular dispersion by a virtually imaged phased array and its application to a wavelength demultiplexer,” *Opt. Lett.*, vol. 21, pp. 366–368, Mar. 1996.

[9] G.-H. Lee, S. Xiao, and A. M. Weiner, “Optical dispersion compensator with >4000-ps/nm tuning range using a virtually imaged phased array (VIPA) and spatial light modulator (SLM),” *IEEE Photon. Technol. Lett.*, vol. 18, no. 17, pp. 1819–1821, Sep. 1, 2006.

[10] S. X. Wang, S. Xiao, and A. M. Weiner, “Broadband, high spectral resolution 2-D wavelength-parallel polarimeter for dense WDM systems,” *Opt. Express*, vol. 13, pp. 9374–9380, Nov. 2005.